

Robust Hybrid Control Using Recurrent Wavelet-Neural-Network Sliding-Mode Controller for Two-Axis Motion Control System

Fayez F. M. El-Sousy

Department of Electrical Engineering
College of Engineering, Salman bin Abdulaziz University
Al-KHARJ, SAUDI ARABIA
Department of Power Electronics and Energy Conversion
Electronics Research Institute
CAIRO, EGYPT
E-mail: f.elsousy@sau.edu.sa

Abstract—In this paper, a robust hybrid control system (RHCS) for achieving high precision motion tracking performance of a two-axis motion control system is proposed. The proposed AHCS incorporating a recurrent wavelet-neural-network controller (RWNNC) and a sliding-mode controller (SMC) to construct a RRWNNSMC. The two-axis motion control system is an x - y table of a computer numerical control machine that is driven by two field-oriented controlled permanent-magnet synchronous motors (PMSMs) servo drives. The RWNNC is used as the main motion tracking controller to mimic a perfect computed torque control law and the SMC controller is designed with adaptive bound estimation algorithm to compensate for the approximation error between the RWNNC and the ideal controller. The on-line learning algorithms of the connective weights, translations and dilations of the RWNNC are derived using Lyapunov stability analysis. A computer simulation and experimental are developed to validate the effectiveness of the proposed RHCS. All control algorithms are implemented in a TMS320C31 DSP-based control computer. The simulation and experimental results using star and four leaves contours are provided to show the effectiveness of the RHCS. The motion tracking performance is significantly improved using the proposed RHCS and robustness to parameter variations, external disturbances, cross-coupled interference and frictional torque can be obtained as well for the two-axis motion control system.

Keywords—Permanent-magnet synchronous motor (PMSM); recurrent wavelet-neural-network (RWNN); sliding-mode control (SMC); x - y table.

I. INTRODUCTION

Computer numerical controlled (CNC) machines have become important elements in modern manufacturing systems [1–3]. The CNC machines generally consist of the mechanical parts with servo drive systems; and the servo controllers that control the multi-axis motion of the mechanical parts. In general, a CNC machine contains an x - y table with a z -axis motion mechanism with each motion axis being driven by an individual actuator system, such as a DC or AC motor. This structure usually leads to the existence of unmodeled dynamics, coupled interferences, unmeasured friction, and disturbances, which often significantly deteriorate the system

performance during a machining process. Many studies that attempt to improve the tracking performance in a machining process by improving the control performance have been reported in the literature [1]–[3].

In recent years, the sliding-mode control (SMC) has received much attention in the control of nonlinear dynamic systems because it can offer beneficial properties such as insensitivity to parameter variations, external load disturbance rejection and fast dynamic response. The attribute of the SMC system is that the controller is switched between two distinct control structures, reaching phase and sliding phase. To keep robustness in the whole sliding-mode control system, several researchers have focused on eliminating the effect of the reaching phase. A sliding curve, chosen as close as possible to the time-optimal trajectory, was proposed in to keep robustness from the initial point to final point. However, the system dynamics are still subject to parameters uncertainties. To solve this problem, a RWNNC controller is added to the SMC to construct a new robust motion controller for two-axis motion control system [4]–[13].

Wavelets have been combined with the neural network to create wavelet–neural–networks (WNNs). It combine the capability of artificial neural networks for learning from process and the capability of wavelet decomposition for identification and control of dynamic systems. The training algorithms for WNN typically converge in a smaller number of iterations than the conventional neural networks. Unlike the sigmoid functions used in the conventional neural networks, the second layer of WNN is a wavelet form, in which the translation and dilation parameters are included. Thus, WNN has been proved to be better than the other neural networks in that the structure can provide more potential to enrich the mapping relationship between inputs and outputs [14]–[21].

In modern manufacturing, the design of the two-axis motion control with high-performance and high-precision machining is substantially required. Moreover, since the dynamic characteristics of the two-axis motion control system are complicated, we propose the robust recurrent wavelet–neural–network sliding-mode controller (RWNNSMC) as a

This work was supported by the Deanship of Scientific Research at Salman bin Abdulaziz University through the grant no. 29/T/33, Saudi Arabia.

new robust motion control system to ensure the desired robustness for the two-axis moving table with high-performance features. The proposed robust controllers (SMC and RWNNSMC) consist of a feed-back SMC in addition to an on-line trained RWNNC. The RWNNC provides an adaptive control signal based on the error between the reference model and the actual output of the motion control system. This error was used to train the connective weights of the RWNNC to provide a good model-following response. Therefore, the motion tracking response can be controlled to follow closely the response of the reference model under a wide range of operating conditions. All adaptive learning algorithms were derived in the sense of Lyapunov stability analysis so that the system tracking stability can be guaranteed in the closed-loop system. Simulation results on star and four leaves reference contours are provided to show the effectiveness of the proposed motion control system.

This paper is organized as follows. Section II presents the field-oriented control (FOC), dynamic analysis of the two-axis motion control system that is driven by two PMSM servo drives and the problem formulation. The description of the robust hybrid control system of the two-axis motion control system is introduced. The design methodology for the robust hybrid control system based on the sliding-mode control and the recurrent wavelet-neural-network are given in Section III. Also, The design procedures and adaptive learning algorithms of the proposed robust hybrid control system are described in Section III. The validity of the design procedure and the robustness of the proposed controller is verified by means of computer simulation and experimental analysis. All of the control algorithms have been developed in a control computer that is based on a TMS320C31 and TMS320P14 DSP DS1102 control board. The dynamic performance of the two-axis motion control system have been studied under load changes and parameter uncertainties. Numerical simulations and experimental results are provided to validate the effectiveness of the proposed hybrid control system in Section IV. Conclusions are introduced in Section V.

II. MODELING OF THE X-Y TABLE DRIVEN BY PMSMS

The x-y table is driven by two MR-J2S-70 A/B servo motor drives and two HC-MFS73B PMSMs manufactured by Mitsubishi. The x-y table with 4mm-screw pitch and 203 mm travel for x-axis and 203 mm travel for y-axis are directly coupled to the rotor of the respective PMSM. The mathematical modeling of the PMSM in the synchronously rotating reference frames can be described as follows. The field oriented control (FOC) technique is employed in order to obtain high torque capability of the PMSM drive through the decoupling control of d-q axes stator currents in the rotor reference frame [12], [13].

$$V_{qs}^r = R_s i_{qs}^r + L_{ss} \frac{d}{dt} i_{qs}^r + \omega_r L_{ss} i_{ds}^r + \omega_r \lambda_m' \quad (1)$$

$$V_{ds}^r = R_s i_{ds}^r + L_{ss} \frac{d}{dt} i_{ds}^r - \omega_r L_{ss} i_{qs}^r \quad (2)$$

The electromagnetic torque can be expressed as:

$$T_e = \frac{3}{2} \cdot \frac{P}{2} \cdot \lambda_m' i_{qs}^r \quad (3)$$

The motion equation of the PMSM can be expressed as:

$$T_e = J_m \left(\frac{2}{P} \right) \frac{d^2}{dt^2} \theta_r + \beta_m \left(\frac{2}{P} \right) \frac{d}{dt} \theta_r + T_L + T_f(v) \quad (4)$$

where V_{qs} , V_{ds} , i_{qs} and i_{ds} are the stator voltages and currents respectively. R_s and L_{ss} are the resistance and self inductance of the stator. θ_r , ω_r , J_m , β_m and P are the rotor position, electrical rotor speed, effective inertia, friction coefficient and the number of poles of the motor respectively. T_e , T_L and $T_f(v)$ are the electromagnetic torque, the load torque and the frictional torque, v is the linear velocity of the x- and y- axes, respectively.

Considering Coulomb friction, viscous friction and Stribeck effect, the friction torque can be formulated as follows.

$$T_f(v) = F_C \operatorname{sgn}(v) + (F_S - F_C) e^{-(v/v_s)^2} \operatorname{sgn}(v) + K_v v \quad (5)$$

where F_C is the Coulomb friction, F_S is the static friction, v_s is the Stribeck velocity parameter, K_v is the coefficient of viscous friction and $\operatorname{sgn}(\cdot)$ is a function. All the parameters in (5) are time varying.

III. RWNN SLIDING-MODE CONTROL SYSTEM

A. Problem Formulation

In order to control the motion of an x-y table, a proposed recurrent-wavelet-neural-network sliding-mode controller is considered. The motions of the x-axis and y-axis are controlled separately. The configuration of the of the proposed motion control system for a single-axis PMSM for the x-y table of CNC machine is shown in Fig. 1. Each axis of the x-y table, which is driven by a field-oriented PMSM servo drive system, can be formulated by rewriting (3) and (4) as follows:

$$\ddot{\theta}_r = -\frac{\beta_m}{J_m} \cdot \frac{P}{2} \dot{\theta}_r + \frac{K_t}{J_m (P/2)} i_{qs}^{r*} - \frac{P}{2} \cdot \frac{1}{J_m} (T_L + T_f(v)) \quad (6)$$

$$\ddot{\theta}_r = A_m \dot{\theta}_r + B_m U(t) + D_m (T_L + T_f(v)) \quad (7)$$

where $U(t) = i_{qs}^{r*}(t)$ is the control effort, $A_m = -(\beta_m / J_m) \cdot (P/2)$, and $B_m = K_t / (J_m \cdot P/2)$, $D_m = -(P/2) \cdot (1 / J_m)$.

Now, assume that the parameters of the motion control system are well known and the external disturbance, the cross-coupled interference and the frictional torque are absent, rewriting (7) can represent the model of the PMSM servo drive system.

$$\ddot{\theta}_r(t) = A_m \dot{\theta}_r(t) + B_m U(t) \quad (8)$$

By considering the dynamics in (7) with parameter variations, disturbance and unpredictable uncertainties, then the cross-coupled interference and the frictional torque are added to the system and the motion equation of the system is modified to:

$$\ddot{\theta}_r(t) = (A_{mn} + \Delta A_m) \dot{\theta}_r(t) + (B_{mn} + \Delta B_m) U(t) + (D_{mn} + \Delta D_m) (T_L + T_f(v)) \quad (9)$$

$$\ddot{\theta}_r(t) = A_{mn} \dot{\theta}_r(t) + B_{mn} U(t) + L(t) \quad (10)$$

where A_{mn} , B_{mn} and D_{mn} are the nominal parameters of A_m , B_m and D_m respectively. ΔA_m , ΔB_m , ΔD_m and T_L are the uncertainties due to mechanical parameters J_m and β_m , and $L(t)$ is the lumped parameter uncertainty and is defined as:

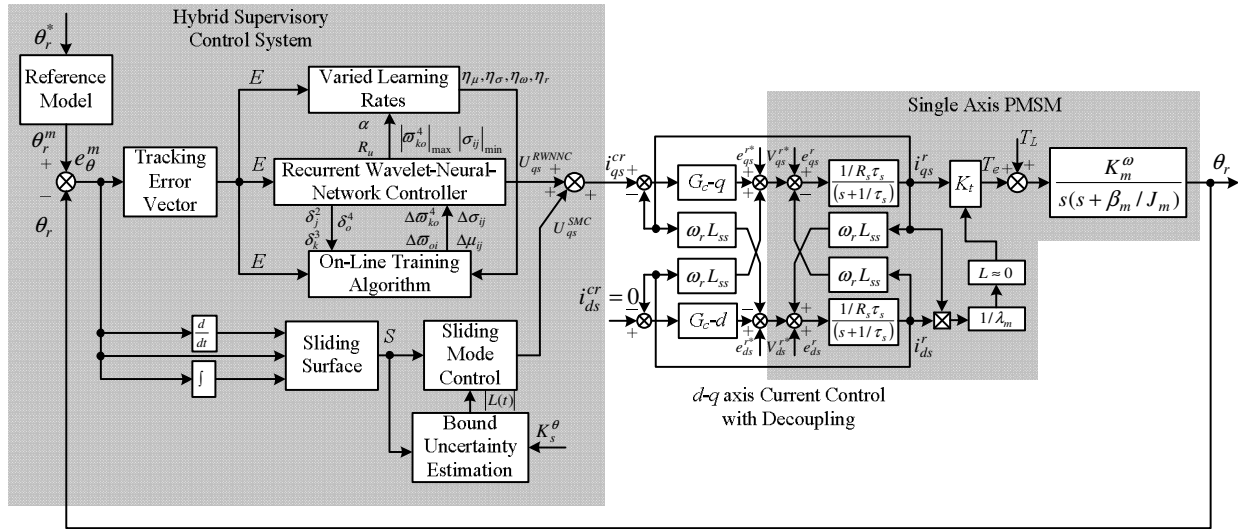


Fig. 1. Robust recurrent wavelet-neural-network sliding-mode control of single-axis PMSM for the two-axis motion control system

$$L(t) = \Delta A_m \dot{\theta}_r(t) + \Delta B_m U(t) + (D_{mn} + \Delta D_m)(T_L + T_f(v)) \quad (11)$$

The bound of the lumped parameter uncertainty is assumed to be given, that is,

$$|L(t)| \leq K^\theta \quad (12)$$

where K^θ is a given positive constants.

To deal with these unpredictable uncertainties and to efficiently control the motion of the x - y table, an RWNSMC control system is proposed for achieving high-precision motion control performance with robust characteristics. The control law is assumed to take the following form:

$$U_{qs}^*(t) = i_{qs}^{rc}(t) = U_{qs}^{RWNNC}(t) + U_{qs}^{SMC}(t) \quad (13)$$

where $U_{qs}^{RWNNC}(t)$ is the RWNNC controller and $U_{qs}^{SMC}(t)$ is the sliding-mode controller.

The inputs to the SMC is the motion error, to construct the sliding surface $S(t)$ and the sliding-mode control law to get the q -axis current command. While the inputs to the RWNNC are the error between the reference model and actual motion and the rate of change of this error, the motion and the rate of change of the motion. Those signals are used to train the connective weights of the RWNNC. The output of the RWNNC is the adaptive control signal, δ_{qs}^{*RWNNC} .

B. Sliding-Mode Motion Controller (SMC)

The structure of the sliding-mode control system of the single-axis PMSM for the x - y table of CNC machine is shown in Fig. 1. The bound of the lumped parameter uncertainty is assumed to be $|L(t)| \leq K^\theta$. The objective is to design a control law so that the motion in the x -axis and y -axis can track any desired command. To achieve this control objective, we can define the error motion function $e_\theta(t) = -(\dot{\theta}_r^*(t) - \dot{\theta}_r(t))$. The sliding surface can be defined as a proportional plus integral plus derivative (PID) performance tracking measure and is given by:

$$S(t) = K_{ps} e_\theta(t) + K_{ds} \dot{e}_\theta(t) + K_{is} \int e_\theta(\tau) d\tau \quad (14)$$

where the positive constants K_{ps} , K_{ds} and K_{is} are positive constants. Differentiating $S(t)$ with respect to time will give:

$$\dot{S}(t) = K_{ps} [\dot{e}_\theta(t) + (K_{ds} / K_{ps}) \ddot{e}_\theta(t) + (K_{is} / K_{ps}) e_\theta(t)] \quad (15)$$

Using the differentiation of the error motion function, $e_\theta(t) = -(\dot{\theta}_r^*(t) - \dot{\theta}_r(t))$, and (10) and substituting into (15) will yield:

$$\begin{aligned} \dot{S}(t) = & K_{ps} [A_{mn} \dot{\theta}_r + B_{mn} U_{qs}^{*SMC} + L(t) - \ddot{\theta}_r^*(t) \\ & + (K_{ds} / K_{ps}) \ddot{e}_\theta(t) + (K_{is} / K_{ps}) e_\theta(t)] \end{aligned} \quad (16)$$

The tracking problem is to find a control law U_{qs}^{*SMC} so that the motion remaining on the sliding surface for all $t > 0$. In the design of the SMC system, the ideal equivalent control law, which determines the dynamics of the drive system on the switching surface, is derived. The ideal equivalent control law is derived from $\dot{S}(t) = 0$. Applying this equality to (16) will provide

$$\dot{S}(t)|_{U_{qs}^{*SMC} = U_{eq}} = 0 \quad (17)$$

Substituting (16) into (17) will yield

$$\begin{aligned} [A_{mn} \dot{\theta}_r + B_{mn} U_{qs}^{*SMC} + L(t) - \ddot{\theta}_r^*(t) + (K_{ds} / K_{ps}) \ddot{e}_\theta(t) \\ + (K_{is} / K_{ps}) e_\theta(t)] = 0 \end{aligned} \quad (18)$$

Solving (18), we can obtain

$$\begin{aligned} U_{eq} = & B_{mn}^{-1} [\ddot{\theta}_r^*(t) - (K_{ds} / K_{ps}) \ddot{e}_\theta(t) \\ & - (K_{is} / K_{ps}) e_\theta(t) - A_{mn} \dot{\theta}_r(t) - L(t)] \end{aligned} \quad (19)$$

Thus, for $\dot{S}(t) = 0$, the dynamic of the system on the sliding surface a $t \geq 0$ is given by

$$\ddot{e}_\theta(t) + (K_{ps} / K_{ds}) \dot{e}_\theta(t) + (K_{is} / K_{ds}) e_\theta(t) = 0 \quad (20)$$

$$\begin{aligned} \dot{S}(t) = & K_{ps}[A_{mn}\dot{\theta}_r + B_{mn}U_{qs}^{*SMC} + L(t) - \ddot{\theta}_r^*(t)] \\ & + (K_{ds}/K_{ps})\ddot{e}_\theta(t) + (K_{is}/K_{ps})e_\theta(t) \end{aligned} \quad (21)$$

The tracking problem is to find a control law U_{qs}^{*SMC} so that the motion remaining on the sliding surface for all $t > 0$. In the design of the SMC system, the ideal equivalent control law, which determines the dynamics of the drive system on the switching surface, is derived. The ideal equivalent control law is derived from $\dot{S}(t) = 0$. Applying this equality to (21) will provide

$$\dot{S}(t) \Big|_{U_{qs}^{*SMC} = U_{eq}} = 0 \quad (22)$$

Substituting (21) into (22) will yield

$$\begin{aligned} [A_{mn}\dot{\theta}_r + B_{mn}U_{qs}^{*SMC} + L(t) - \ddot{\theta}_r^*(t) + (K_{ds}/K_{ps})\ddot{e}_\theta(t) \\ + (K_{is}/K_{ps})e_\theta(t)] = 0 \end{aligned} \quad (23)$$

Solving (23), we can obtain

$$\begin{aligned} U_{eq} = & B_{mn}^{-1}[\ddot{\theta}_r^*(t) - (K_{ds}/K_{ps})\ddot{e}_\theta(t) \\ & - (K_{is}/K_{ps})e_\theta(t) - A_{mn}\dot{\theta}_r(t) - L(t)] \end{aligned} \quad (24)$$

Thus, for $\dot{S}(t) = 0$, the dynamic of the system on the sliding surface a $t \geq 0$ is given by

$$\ddot{e}_\theta(t) + (K_{ps}/K_{ds})\dot{e}_\theta(t) + (K_{is}/K_{ds})e_\theta(t) = 0 \quad (25)$$

To ensure the system performance, designed by (25), in spite of the existence the uncertain dynamics, a new sliding-mode control law is proposed in the following section.

From (23) and the lumped parameter uncertainty condition $|L(t)| \leq K^\theta$, the sliding-mode control objective is given by:

$$U_{qs}^{*SMC}(t) = i_{qs}^{r*}(t) = U_{qs}^{DP} + U_{qs}^{TE} + U_{qs}^{SS} \quad (26)$$

$$\begin{aligned} U_{qs}^{*SMC}(t) = & i_{qs}^{r*}(t) = B_{mn}^{-1}[\ddot{\theta}_r^*(t) - (K_{ds}/K_{ps})\ddot{e}_\theta(t) \\ & - (K_{is}/K_{ps})e_\theta(t)] - B_{mn}^{-1}[A_{mn}\dot{\theta}_r(t) - B_{mn}^{-1}[K^\theta \operatorname{sgn}(S(t))] \end{aligned} \quad (27)$$

where $\operatorname{sign}(\cdot)$ is a sign function. The first term in (27), U_{qs}^{DP} , describes the desired system performance, the second term, U_{qs}^{TE} , is a torque estimator which is able to compensate for the nonlinear effect in the PMSM model, while the third one, U_{qs}^{SS} , keeps the single-axis PMSM for the x-y table of CNC machine dynamics on the sliding surface $S(t)=0$ for all the time.

Theorem 1: The globally asymptotic stability of (21) is guaranteed if the sliding-mode control law is designed as (27).

Proof: Define the Lyapunov function candidate as:

$$V(S(t)) = \frac{1}{2} S^2(t) \quad (28)$$

Taking the derivative of the Lyapunov function and using (27), we can get

$$\begin{aligned} \dot{V}(S(t)) = & S(t)\dot{S}(t) \\ = & S(t)K_{ps}[A_{mn}\dot{\omega}_r + B_{mn}U_{qs}^{*SMC} + L(t) - s\ddot{\omega}_r^*(t) \\ & + (K_{ds}/K_{ps})\ddot{e}_\omega(t) + (K_{is}/K_{ps})e_\omega(t)] \\ = & S(t)L(t) - |S(t)|K_s^\theta \\ \leq & |S(t)||L(t)| - |S(t)|K_s^\theta \\ \leq & -|S(t)|[K_s^\theta - |L(t)|] < 0 \end{aligned} \quad (29)$$

Therefore, the sliding condition can be assured throughout the whole control period. According to the Lyapunov theorem [4-6], the globally asymptotic stability of the sliding-mode control system can be guaranteed.

The major advantage of the sliding-mode control is its insensitivity to parameter variations and external disturbance, the cross-coupled interference and the frictional torque once in the switching surface. To keep the trajectory in the sliding surface, the selection of the control gain, K^θ , is very important due to its significant effect on the magnitude of the lumped parameter uncertainties of the system and hence its performance. The incorrect selection of this control gain will yield to the deviation from the sliding surface and causing chattering phenomena. If the uncertainties are absent, once the switching surface is reached, a very small positive value of the control gain, K^θ , would be sufficient to keep the trajectory on the sliding surface and the amplitude of the chattering is small. However, when the uncertainties are present, deviations from the sliding surface will occur and causing a large amount of chattering. To solve this problem an adaptive controller using RWNN is augmented to the SMC to preserve the desired tracking motion response under parameter uncertainties and external disturbances. In the following section, the RWNNC is introduced.

C. Recurrent Wavelet-Neural-Network Motion Controller (RWNNC)

1) Recurrent Wavelet-Neural-Network (RWNN) Structure

The architecture of the proposed four-layers RWNN is shown in Fig. 2, which comprises an input layer (the i layer), a mother wavelet layer (the j layer), a wavelet layer (the k layer) and an output layer (the o layer), is adopted to implement the RWNNC in this project. Moreover, z^{-1} represents a time-delay and the output of the RWNN is recurrent to the input layer through a time delay. The signal propagation and the basic function in each layer of the RWNN are introduced as follows.

Layer 1: Input Layer

The nodes in layer 1 transmit the input signals to the next layer. The input variables are the error signal, e_θ^{mf} , and the rate of change of the rotor speed, $K_\theta\dot{\theta}_r$. For every node i in the input layer, the input and the output of the RWNN can be represented as:

$$net_i^1 = \prod_o x_i^1(N)\varpi_{oi}y_o^4(N-1) \quad (30)$$

$$y_i^1(N) = f_i^1(net_i^1(N)) = net_i^1(N) \quad i = 1, 2 \quad (31)$$

$$x_1^1 = e_\theta^{mf}(t) \quad \text{and} \quad x_2^1 = K_\theta\dot{\theta}_r(t) \quad (32)$$

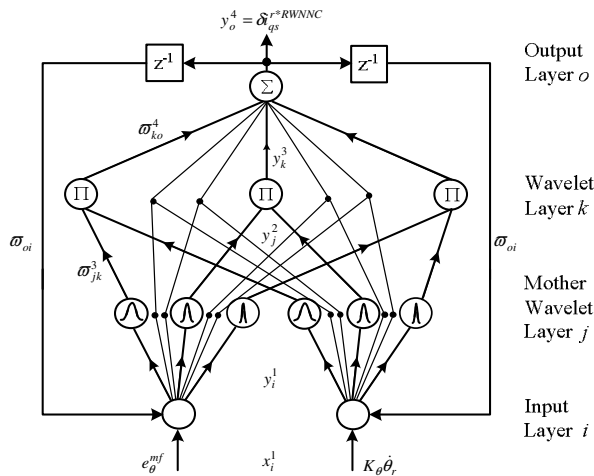


Fig. 2. Four-layer recurrent wavelet–neural–network (RWNN) structure

where x_i^1 represents the i th input to the node of layer 1, N denotes the number of iterations, ω_{oi} is the recurrent weights for the units of the output layer and y_o^4 is the output of the RWNN.

Layer 2: Mother Wavelet Layer

A family of wavelets is constructed by translations and dilations performed on the mother wavelet. In the mother wavelet layer each node performs a wavelet ϕ that is derived from its mother wavelet. There are many kind of wavelets that can be used in RWNN. In this project, the first derivative of the Gaussian wavelet function $\phi(x) = -x \exp(-x^2/2)$, is adopted as a mother wavelet. For the j th node

$$net_j^2(N) = -\frac{x_i^2 - \mu_{ij}}{\sigma_{ij}} \quad (33)$$

$$y_j^2(N) = f_j^2(net_j^2(N)) = \phi_j(net_j^2(N)), j = 1, \dots, n \quad (34)$$

where μ_{ij} and σ_{ij} are the translation and dilations in the j th term of the i th input x_i^2 to the node of mother wavelet layer and n is the total number of the wavelets with respect to the input nodes.

Layer 3: Wavelet Layer

Each node k in layer 3 (wavelet layer) is denoted by Π , which multiplies the incoming signal and outputs the result of the product. For the k th nodes:

$$net_k^3(N) = \prod_j \omega_{jk}^3 x_j^3(N) \quad (35)$$

$$y_k^3(N) = f_k^3(net_k^3(N)) = net_k^3(N) \quad k = 1, \dots, m \quad (36)$$

where x_j^3 represents the j th input to the node of the wavelet layer (layer 3), ω_{jk}^3 is the weights between the mother wavelet layer and the wavelet layer. These weights are also assumed to be unity; and $m = (n/i)$ is the number of wavelets if each input node has the same mother wavelet nodes.

Layer 4: Output Layer

The single node o in the output layer is denoted by Σ , which computes the overall output as the summation of all incoming signals.

$$net_o^4 = \sum_k \omega_{ko}^4 x_k^4(N) \quad (37)$$

$$y_o^4(N) = f_o^4(net_o^4(N)) = net_o^4(N) \quad o = 1 \quad (38)$$

$$y_o^4 = U_{qs}^{*RWNNC}(t) = \delta_{qs}^{r*RWNNC}(t) \quad (39)$$

where the connecting weight ω_{ko}^4 is the output action strength of the o th output associated with the k th wavelet and x_k^4 represents the k th input to the node of output layer.

The control problem is to design the RWNNC to improve the convergence of the tracking error for the for the x - y table of CNC machine.

2) On-line Training Algorithm for RWNNC

The essential part of the learning algorithm for an RWNN concerns how to obtain a gradient vector in which each element in the learning algorithm is defined as the derivative of the energy function with respect to a parameter of the network using the chain rule. Since the gradient vector is calculated in the direction opposite to the flow of the output of each node, the method is generally referred to back-propagation learning rule, because the gradient vector is calculated in the direction opposite to the flow of the output of each node [7-13]. To describe the on-line learning algorithm of the RWNNC using the supervised gradient descent method, the energy function is chosen as:

$$E_{\theta} = \frac{1}{2} (\theta_r^{mf} - \theta_r)^2 = \frac{1}{2} (e_{\theta}^{mf})^2 \quad (40)$$

Layer 4:

In the output layer (layer 4), the error term to be propagated is calculated as:

$$\delta_o^4 = -\frac{\partial E_{\theta}}{\partial y_o^4} = \left[-\frac{\partial E_{\theta}}{\partial e_{\theta}^{mf}} \cdot \frac{\partial e_{\theta}^{mf}}{\partial net_o^4} \right] = \left[-\frac{\partial E_{\theta}}{\partial e_{\theta}^{mf}} \cdot \frac{\partial e_{\theta}^{mf}}{\partial \theta_r} \cdot \frac{\partial \theta_r}{\partial y_o^4} \right] \quad (41)$$

The weight is updated by the amount:

$$\Delta \omega_{ko}^4 = -\eta_{\theta} \frac{\partial E_{\theta}}{\partial \omega_{ko}^4} = \left[-\eta_{\theta} \frac{\partial E_{\theta}}{\partial y_o^4} \right] \left(\frac{\partial y_o^4}{\partial net_o^4} \cdot \frac{\partial net_o^4}{\partial \omega_{ko}^4} \right) = \eta_{\theta} \delta_o^4 x_k^4 \quad (42)$$

where η_{θ} is the learning rate parameter of the connecting weights of the output layer of the RWNNC.

The weights of the output layer (layer 4) are updated according to the following equation.

$$\omega_{ko}^4(N+1) = \omega_{ko}^4(N) + \Delta \omega_{ko}^4 = \omega_{ko}^4(N) + \eta_{\theta} \delta_o^4 x_k^4 \quad (43)$$

where N denotes the number of iterations.

Layer 3:

In wavelet layer (layer 3), only the error term needs to be computed and propagated because the weights in this layer are unity.

$$\delta_k^3 = -\frac{\partial E_\theta}{\partial net_k^3} = \left[-\frac{\partial E_\theta}{\partial y_o^4} \left(\frac{\partial y_o^4}{\partial net_o^4} \frac{\partial net_o^4}{\partial y_k^3} \frac{\partial y_k^3}{\partial net_k^3} \right) \right] = \delta_o^4 \omega_{ko}^4 \quad (44)$$

Layer 2:

In the mother wavelet layer (layer 2), the multiplication operation is done. The error term is calculated as follows:

$$\delta_j^2 = -\frac{\partial E_\theta}{\partial net_j^2} = \left(-\frac{\partial E_\theta}{\partial y_o^4} \frac{\partial y_o^4}{\partial net_o^4} \frac{\partial net_o^4}{\partial y_j^3} \frac{\partial y_j^3}{\partial net_j^2} \right) \left(\frac{\partial net_k^3}{\partial y_j^2} \frac{\partial y_j^2}{\partial net_j^2} \right) = \sum_k \delta_k^3 y_k^3 \quad (45)$$

The update law of μ_{ij} is given by:

$$\Delta \mu_{ij} = -\eta_\mu \frac{\partial E_\theta}{\partial \mu_{ij}} = \left[-\eta_\mu \frac{\partial E_\theta}{\partial y_j^2} \frac{\partial y_j^2}{\partial net_j^2} \frac{\partial net_j^2}{\partial \mu_{ij}} \right] = -\eta_\mu \frac{\delta_j^2}{\sigma_{ij}} \quad (46)$$

The update law of σ_{ij} is given by:

$$\Delta \sigma_{ij} = -\eta_\sigma \frac{\partial E_\theta}{\partial \sigma_{ij}} = \left[-\eta_\sigma \frac{\partial E_\theta}{\partial y_j^2} \frac{\partial y_j^2}{\partial net_j^2} \frac{\partial net_j^2}{\partial \sigma_{ij}} \right] = \eta_\sigma \delta_j^2 \left(\frac{\mu_{ij} - x_i^2}{(\sigma_{ij})^2} \right) \quad (47)$$

where η_μ and η_σ are the learning rate parameters of the translation and dilation of the mother wavelet. The translation and dilation of the mother wavelet are updated as follows:

$$\mu_{ij}(N+1) = \mu_{ij}(N) + \Delta \mu_{ij} \quad (48)$$

$$\sigma_{ij}(N+1) = \sigma_{ij}(N) + \Delta \sigma_{ij} \quad (49)$$

The update law of the recurrent weight ω_{oi} can be obtained by the following equation:

$$\Delta \omega_{oi} = -\eta_r \frac{\partial E_\theta}{\partial \omega_{oi}} = \left[-\eta_r \frac{\partial E_\theta}{\partial net_j^2} \cdot \frac{\partial net_j^2}{\partial y_i^1} \cdot \frac{\partial y_i^1}{\partial net_i^1} \cdot \frac{\partial net_i^1}{\partial \omega_{oi}} \right] = \sum_j \eta_r \delta_j^2 \left(\frac{2(\mu_{ij} - x_i^2(N))}{(\sigma_{ij})^2} \right) x_i^1(N) y_o^4(N-1) \quad (50)$$

where η_r is the learning rate parameters of the recurrent weights. The recurrent weights updated as follows:

$$\omega_{oi}(N+1) = \omega_{oi}(N) + \Delta \omega_{oi} \quad (51)$$

To overcome the problem of uncertainties of the motion system due to parameter variations and to increase the on-line learning rate of the network parameters, a control law is proposed as follows.

$$\delta_o^4 = e_\theta^{mf} + K_\theta \ddot{\theta}_r \quad (52)$$

Selection of the values for the learning rates η_θ , η_μ , η_σ and η_r has a significant effect on the network performance. In order

to train the RWNN, adaptive learning rates, which guarantee the convergence of tracking error based on the analyses of a discrete-type Lyapunov function, are derived in [7].

IV. NUMERICAL SIMULATION AND EXPERIMENTAL RESULTS

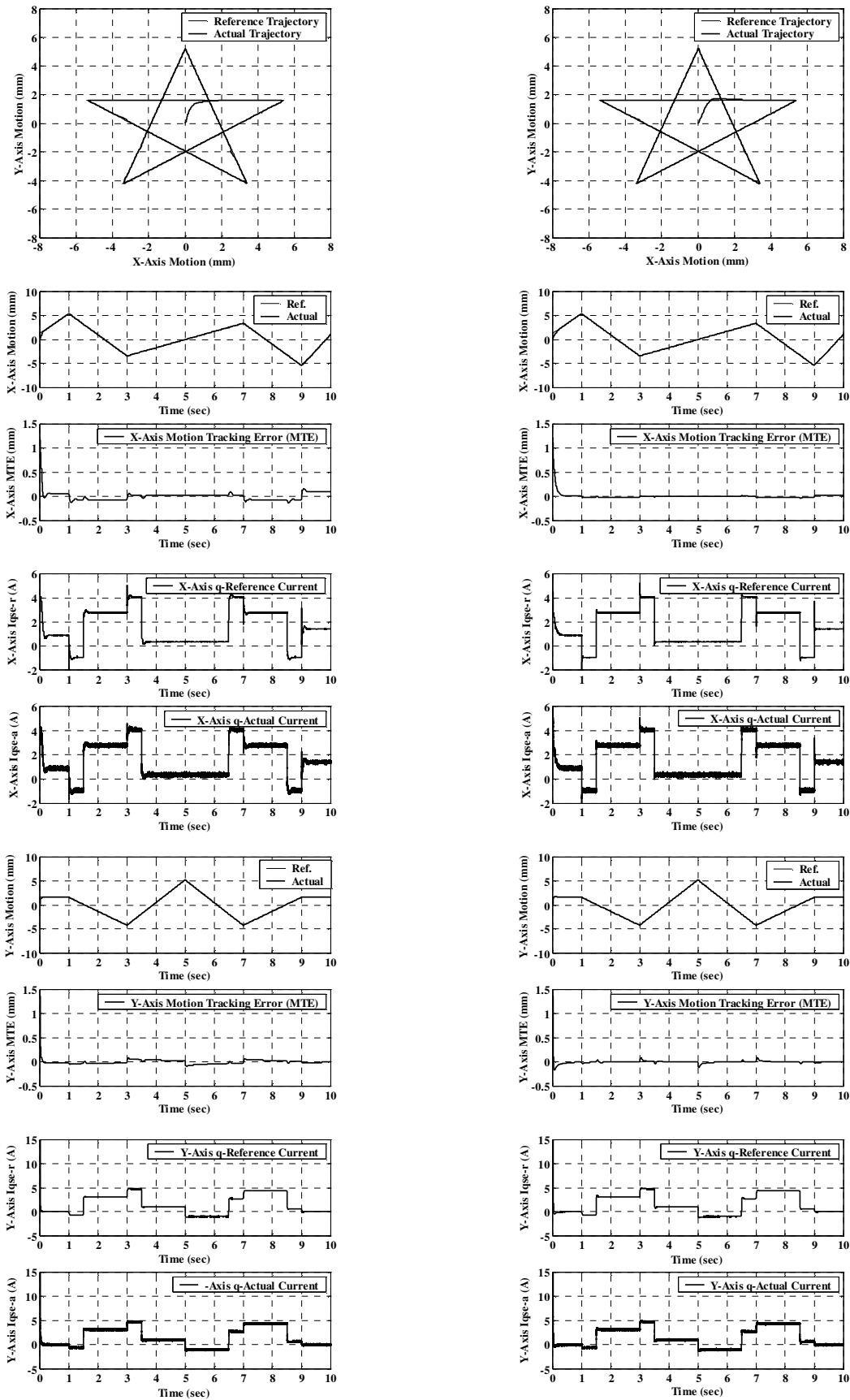
In order to investigate the effectiveness of the proposed tracking control scheme, the simulation and experimentation of the proposed control schemes are carried out using MATLAB/SIMULINK package based on the control system shown in Fig. 1. A DSP control board dSPACE DS1102, that is based on a TMS320C31 and TMS320P14 DSPs, is installed in the control computer which includes multi-channels of ADC, DAC, PIO and encoder interface circuits. Digital filter and frequency multiplied by four circuits are built into the encoder interface circuits to increase the precision of the speed and the position feedback signals and coordinate transformations. The sampling rate is chosen as 200 μ s and hence, the carrier frequency of the PWM inverter is 5 kHz. The control interval of the motion control loop is set at 1 ms. The current-regulated PWM VSI is implemented using Mitsubishi intelligent power module (IPM) using IGBTs with rating of 50A, 1200V and a switching frequency of 15 kHz and driven by a six SEMIKRON IGBT drivers. The DC-link LC filter components are an inductor of iron powder core with 250 μ H and a polypropylene-film capacitor with 5 μ F.

A. Numerical Simulation of the Two-Axis Motion Control System

In this section, the proposed RWNN sliding-mode control will be applied to control the motion of the two-axis moving system. The feedback gain vector K is designed such that the system is stable. The gain $K = [k_1 \ k_2] = [10 \ 50]^T$. The parameters of the proposed RWNN sliding-mode control system are given in the following:

$$K_{ps} = 50, \quad K_{is} = 500, \quad K_{ds} = 1, \quad K_s^\theta = 35, \quad \alpha = 7, \quad R_u = 0.1$$

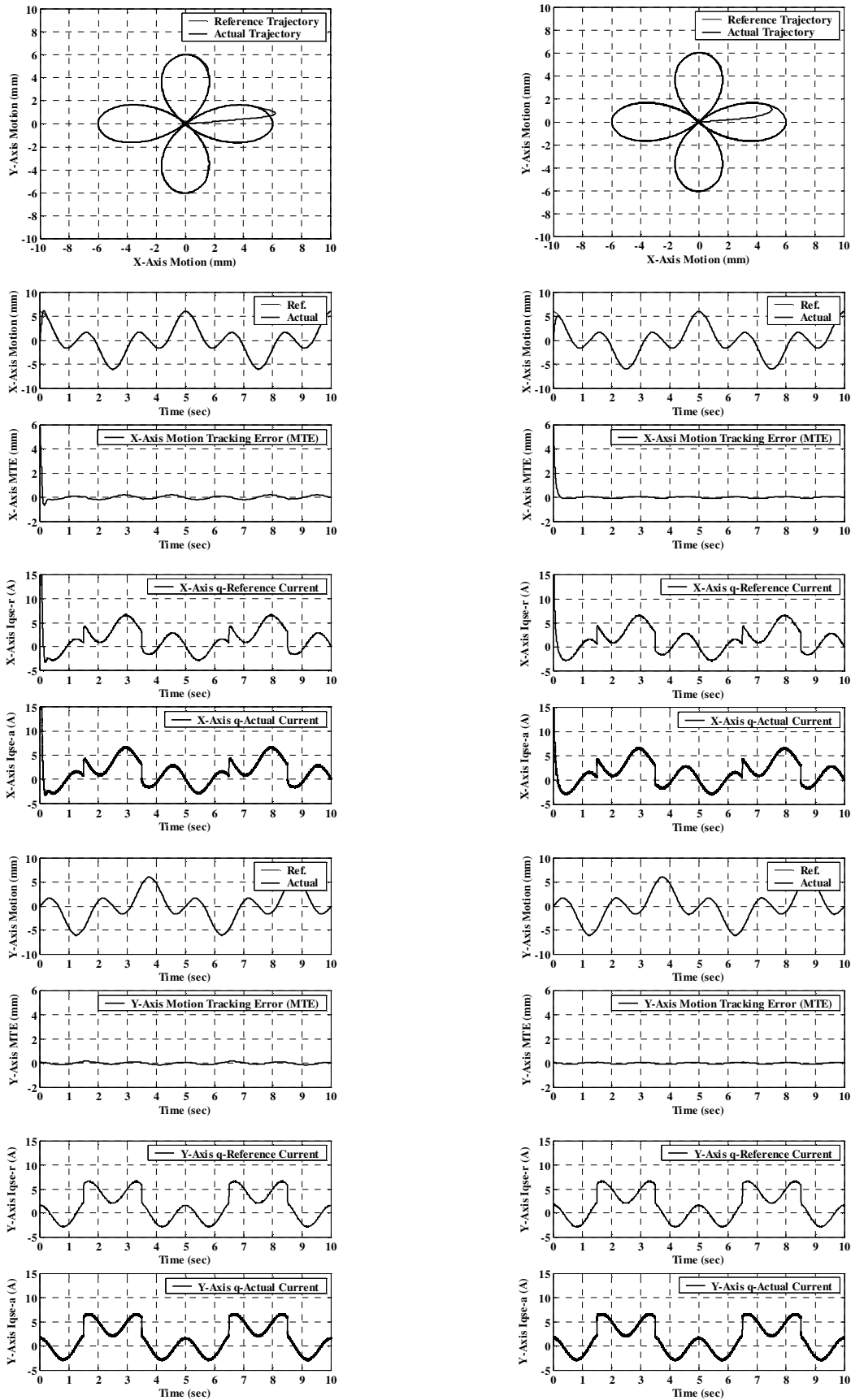
The simulated results of the proposed RWNN sliding-mode control system are demonstrated as follows. First, the sliding-mode control is applied to control the two-axis motion control system. The tracking responses of the x - y table, the control efforts, and the tracking errors of x -axis and y -axis due to the star contour at subsequent loading are depicted in Fig. 3(a). Moreover, the tracking responses of the x - y table, the control efforts, and the tracking errors of x -axis and y -axis due to four leaves contour at subsequent are depicted in Fig. 4(a). To improve the control performance, the proposed RWNN sliding-mode control system is applied to control the two-axis motion control system. The tracking responses of the x - y table, the control efforts, and the tracking errors of x -axis and y -axis due to the star contour at subsequent are depicted in Fig. 3(b). Moreover, the tracking responses of the x - y table, the control efforts, and the tracking errors of x -axis and y -axis due to four leaves contour at subsequent are depicted in Figs. 4(b). From the simulated results, good tracking responses can be achieved at both cases of parameter variations. Furthermore, robust control characteristics can be obtained with regard to parameter variation. Therefore, the proposed RWNN sliding-mode control system is more suitable to control an x - y table of a CNC machine when uncertainties occur in the reference trajectories.



(a) Sliding-mode control

(b) RWNN sliding-mode control

Fig. 3. Simulation results of the dynamic response of the two-axis motion control system with star contour.



(a) Sliding-mode control

(b) RWNN sliding-mode control

Fig. 4. Simulation results of the dynamic response of the two-axis motion control system with four leaves contour.

B. Experimental Results of the Two-Axis Motion Control System

To further verify the performance of the proposed control schemes applied to the two-axis motion control system in practical applications, some experimental results are introduced. The experimental results of the dynamic performance for the proposed SMC and RWNSMC controllers due to star and four leavers reference contour are predicted in Figs. (5-6), respectively. First, the sliding-mode control is applied to control the two-axis motion control system. The tracking responses of the x - y table, the control efforts, and the tracking errors of x -axis and y -axis due to the star contour at subsequent loading are depicted in Fig. 5(a). Moreover, the tracking responses of the x - y table, the control efforts, and the tracking errors of x -axis and y -axis due to four leaves contour at subsequent are depicted in Fig. 6(a). To improve the control performance, the proposed RWNN sliding-mode controller is applied to control the two-axis motion control system. The tracking responses of the x - y table, the control efforts, and the tracking errors of x -axis and y -axis due to the star contour at subsequent are depicted in Fig. 5(b). Moreover, the tracking responses of the x - y table, the control efforts, and the tracking errors of x -axis and y -axis due to four leaves contour at subsequent are depicted in Figs. 6(b). From the experimental results, good tracking responses can be achieved at both cases of parameter variations. Furthermore, robust control characteristics can be obtained with regard to parameter variation. Therefore, the proposed RWNN sliding-mode control system is more suitable to control an x - y table of a CNC machine when uncertainties occur in the reference trajectories. It is obvious that the performance of the two-axis motion control system using the RHCS is improved greatly. Thus, it can be verified that the proposed RHCS can satisfy the accuracy requirements and is more suitable in the tracking control of the two-axis motion control system for practical applications.

V. CONCLUSIONS

This paper proposed a robust RWNN sliding-mode motion controllers to control an x - y table composed of two PMSM servo drives under field-orientation which guarantee the robustness in the presence of parameter uncertainties. The theoretical bases and stability analyses of the proposed control system were described in detail. Furthermore, a simple adaptive algorithm was utilized to adjust the uncertainty term in the sliding-mode controller according to the function of the sliding surface. Therefore, the motion tracking response in x - y axis can be controlled to follow closely the response of the reference contour under a wide range of operating conditions. Simulation and experimental results have shown that the proposed hybrid control system grant robust tracking response in the presence of parameter uncertainties and external disturbances. Moreover, simulations and experimentations were carried out using star and four leavers reference contour trajectories to testify the effectiveness of the proposed controllers.

ACKNOWLEDGMENT

The author would like to acknowledge the financial support of the Deanship of Scientific Research at Salman bin Abdulaziz University, Saudi Arabia through its grant no. 29/T/33.

REFERENCES

- [1] M. P. Groover, *Fundamentals of Modern Manufacturing: Materials, Process, and Systems*. Upper Saddle River, NJ: Prentice-Hall, 1996.
- [2] D. I. Kim and C. H. Yim, "All digital high performance controller for spindle motor in CNC machine tool," in *Proc. IEEE Int. Conf. Elect. Mach. Drives*, 1997, pp. MC2/2.1–MC2/2.3.
- [3] D. Hanafi, M. Tordon, and J. Katupitiya, "An active axis control system for a conventional CNC machine," in *Proc. IEEE/ASME Int. Conf. Advanced Intell. Mechatronics*, 2003, pp. 1188–1193.
- [4] J.L. Sosa, M. Castilla, J. Miret, L.G. de Vicuna, L.S. Moreno, "Sliding-Mode Input–Output Linearization Controller for the DC/DC ZVS CLL-T Resonant Converter," *IEEE Trans. on Industrial Electronics*, vol. 59, no. 3, pp. 1554–1564, Mar 2012..
- [5] Z. Qiao, T. Shi, Y. Wang, Y. Yan, C. Xia, X. He " New Sliding-Mode Observer for Position Sensorless Control of Permanent-Magnet Synchronous Motor," *IEEE Trans. on Industrial Electronics*, vol. 60, no. 2, pp. 710–719, Feb 2013..
- [6] E. Kayacan, O. Cigdem, O. Kaynak, " Sliding Mode Control Approach for Online Learning as Applied to Type-2 Fuzzy Neural Networks and Its Experimental Evaluation," *IEEE Trans. on Industrial Electronics*, vol. 59, no. 9, pp. 3510–3520, Sep 2012.
- [7] Qingsong Xu, Yangmin Li, " Micro-/Nanopositioning Using Model Predictive Output Integral Discrete Sliding Mode Control," *IEEE Trans. on Industrial Electronics*, vol. 59, no. 2, pp. 1161–1170, Feb 2012.
- [8] L.M. Capisani, A. Ferrara, A. Ferreira de Loza, L.M. Fridman, " Manipulator Fault Diagnosis via Higher Order Sliding-Mode Observers," *IEEE Trans. on Industrial Electronics*, vol. 59, no. 10, pp. 3979–3986, Oct 2012.
- [9] M. Canale, L. Fagiano, A. Ferrara, C. Vecchio, "Vehicle Yaw Control via Second-Order Sliding-Mode Technique," *IEEE Trans. Ind. Electron.*, vol. 55, no. 11, pp. 3908–3916, Nov. 2008.
- [10] L.M. Capisani, A. Ferrara, " Trajectory Planning and Second-Order Sliding Mode Motion/Interaction Control for Robot Manipulators in Unknown Environments," *IEEE Trans. on Industrial Electronics*, vol. 59, no. 8, pp. 3189–3198, Aug 2012.
- [11] Jun Hu, Zidong Wang, Huijun Gao, L.K. Stergioulas, " Robust Sliding Mode Control for Discrete Stochastic Systems With Mixed Time Delays, Randomly Occurring Uncertainties, and Randomly Occurring Nonlinearities," *IEEE Trans. on Industrial Electronics*, vol. 59, no. 7, pp. 3008–3015, Jul 2012.
- [12] F. F. M. El-Sousy, "An Intelligent Model-Following Sliding-Mode Position Controller for PMSM Servo Drives," *4th IEEE International Conference on Mechatronics*, Kumamoto, Japan, May 8–10, 2007.
- [13] F. F. M. El-Sousy, "Robust Tracking Control Based on Intelligent Sliding-Mode Model-Following Position Controller for PMSM Servo Drive," *Journal of Power Electronics, JPE*, vol. 7, no. 2, pp. 159–173, April 2007.
- [14] B. Delyon, A. Juditsky, and A. Benveniste, "Accuracy analysis for wavelet approximations," *IEEE Trans. on Neural Networks*, vol. 6, pp. 332–348, March 1995.
- [15] C. F. Chen and C. H. Hsiao, "Wavelet approach to optimizing dynamic systems," *Proc. IEE—Control Theory Application*, vol. 146, no. 2, pp. 213–219, March 1999.
- [16] Q. Zhang and A. Benveniste, "Wavelet networks," *IEEE Trans. on Neural Networks*, vol. 3, pp. 889–898, Nov. 1992.
- [17] J. Zhang, G. G. Walter, Y. Miao, and W. N. W. Lee, "Wavelet neural networks for function learning," *IEEE Trans. on Signal Processing*, vol. 43, pp. 1485–1496, June 1995.
- [18] Z. Zhang and C. Zhao, "A fast learning algorithm for wavelet network and its application in control," *2007 IEEE International Conference on Control and Automation*, pp. 1403–1407, China, May 30– June 1, 2007.
- [19] N. Sureshbabu and J. A. Farrell, "Wavelet-based system identification for nonlinear control," *IEEE Trans. on Automatic Control*, vol. 44, no. 2, pp. 412–417, Feb. 1999.
- [20] S. A. Billings and H. L. Wei, "A new class of wavelet networks for nonlinear system identification," *IEEE Trans. on Neural Network*, vol. 16, no. 4, pp. 862–874, July 2005.
- [21] D. Giaouris, J.W. Finch, O.C. Ferreira, R.M. Kennel, G. M. El-Murr, "Wavelet Denoising for Electric Drives," *IEEE Trans. on Industrial Electronics*, vol. 55, No. 2, pp. 543–550, Feb. 2008.

**Creative Commons Attribution License 4.0
 (Attribution 4.0 International, CC BY 4.0)**

This article is published under the terms of the Creative Commons Attribution License 4.0

https://creativecommons.org/licenses/by/4.0/deed.en_US

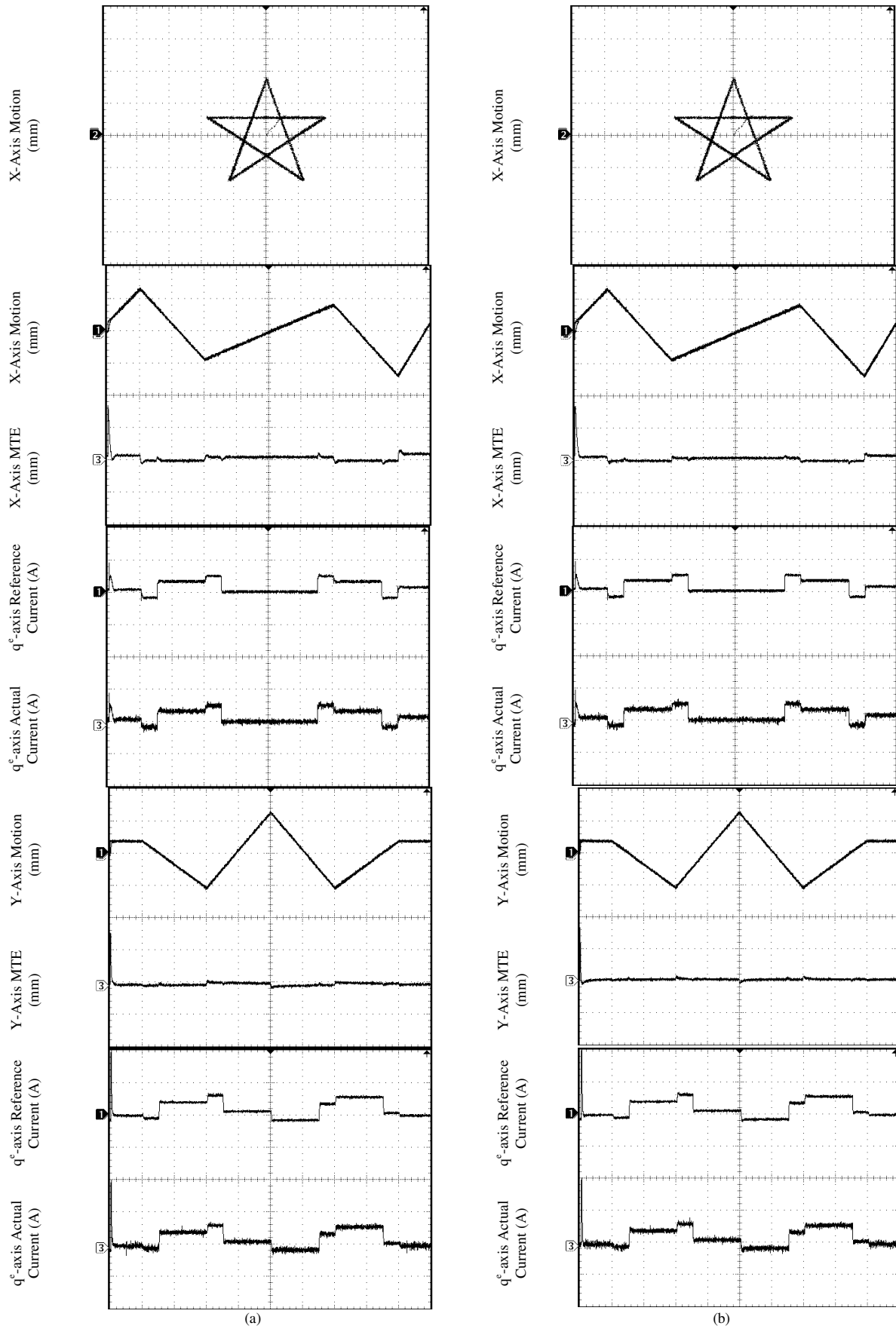


Fig. 5. Experimental results of the dynamic response of the two-axis motion control system using star reference contours.

(a) Using SMC tracking controller

(b) Using RHCS with RWNN tracking controller

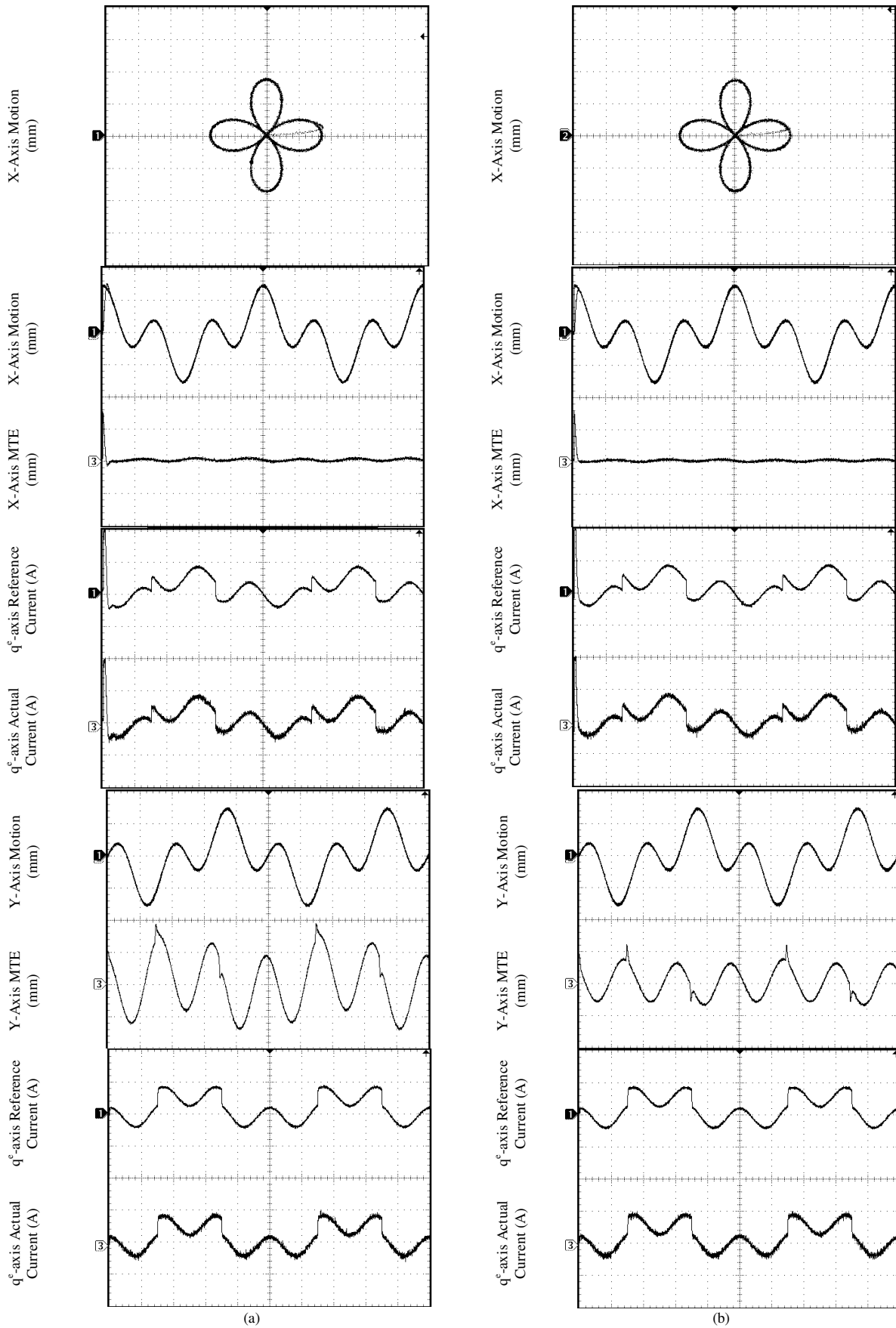


Fig. 6. Experimental results of the dynamic response of the two-axis motion control system using star reference contours.
 (a) Using SMC tracking controller
 (b) Using RHCS with RWNN tracking controller